ample, and to Dr. L. Jacques, from the Université catholique de Louvain, for his comments on numerical integration on a sphere.

REFERENCES

[1] A. Roederer, "Etude des réseaux finis de guides rectangulaires à parois épaisses," *L'onde électrique*, vol. 51, pp. 854–861, Nov. 1971.
[2] A. K. Skrivervik and J. R. Mosig, "Analysis of finite phased arrays of microstrip patches," *IEEE Trans. Antennas Propag.*, vol. 41, pp. 1105–1114, Aug. 1993.
[3] A. Neto, S. Maci, G. Vecchi, and M. Sabbadini, "A truncated floquet wave diffraction method for the full-wave analysis of large phased arrays–Part II: Generalization to 3-D cases," *IEEE Trans. Antennas Propagat.*, vol. 48, pp. 601–611, Apr. 2000.
[4] C. Craeye and X. Dardenne, "Element pattern analysis of wideband arrays with the help of a finite-by-infinite array approach," *IEEE Trans. Antennas Propag.*, vol. 54, pp. 519–526, Feb. 2006.
[5] R. Coifman, V. Rokhlin, and S. Wandzuraz, "The fast multipole method for the wave equation: A pedestrian prescription," *IEEE Antennas Propag. Mag.*, vol. 35, pp. 7–12, Jun. 1993.
[6] T. J. Cui, W. C. Chew, G. Chen, and J. M. Song, "Efficient MLFMA, RPFMA and FAFFA algorithms for EM scattering by very large structures," *IEEE Trans. Antennas Propag.*, vol. 52, pp. 759–770, Mar. 2004.
[7] P. Janpugdee, P. H. Pathak, P. Mahachoklertwattana, and R. J. Burkholder, "An accelerated DFT-MoM for the analysis of large finite periodic antenna arrays," *IEEE Trans. Antennas Propag.*, vol. 54, pp. 279–283, Jan. 2006.
[8] W. B. Lu, T. J. Cui, X. X. Yin, Z. G. Qian, and W. Hong, "Fast algorithms for large-scale periodic structures using subentire domain basis functions," *IEEE Trans. Antennas Propag.*, vol. 53, pp. 1154–1162, Mar. 2005.
[9] C. Craeye, A. G. Tijhuis, and D. H. Schaubert, "An efficient MoM formulation for finite-by-infinite arrays of two-dimensional antennas arranged in a three-dimensional structure," *IEEE Trans. Antennas Propag.*, vol. 52, pp. 271–282, Jan. 2004.
[10] J. Yeo, V. Prakash, and R. Mittra, "Efficient analysis of a class of microstrip antennas using the Characteristic basis function method (CBFM)," *Microw. Opt. Technol. Lett.*, vol. 39, pp. 456–464, Dec. 2003.
[11] J. X. Wan, J. Lei, and C. H. Liang, "An efficient analysis of large-scale periodic microstrip antenna arrays using the characteristic basis function method," *Prog. Eletromag. Res.*, vol. 50, pp. 61–81, Aug. 2005.
[12] E. Suter and J. R. Mosig, "A subdomain multilevel approach for the efficient MoM analysis of large planar antennas," *Microw. Opt. Technol. Lett.*, vol. 26, pp. 270–277, Mar. 2000.
[13] L. Matekovits, G. Vecchi, G. Dassano, and M. Orefice, "Synthetic function analysis of large printed structures: The solution space sampling approach," in *Proc. IEEE Antennas Propagat. Soc. Int. Symp.*, Boston, MA, Jun. 2001, pp. 568–571.
[14] C. Craeye, "New analysis method for finite periodic structures combining macro basis functions and multipole approaches," presented at the Proc. IEEE Symp. Antennas Propagat., Albuquerque, NM, Jul. 9–14, 2006C. Craeye, "New analysis method for finite periodic structures combining macro basis functions and multipole approaches," in *Proc. IEEE Symp. Antennas Propagat.*, Albuquerque, NM, Jul. 9–14, 2006.
[15] V. Prakash and R. Mittra, "Characteristic basis function method: a new technique for efficient solution of method of moments matrix equations," *Microw. Opt. Technol. Lett.*, vol. 36, pp. 95–100, Jan. 2003.
[16] O. M. Bucci and G. Franceschetti, "On the spatial bandwidth of scattered fields," *IEEE Trans. Antennas Propag.*, vol. 35, pp. 1445–1445, Dec. 1987.
[17] A. Boag and C. Letrou, "Fast radiation pattern evaluation for lens and reflector antennas," *IEEE Trans. Antennas Propag.*, vol. 51, pp. 1063–1068, May 2003.
[18] J. R. Driscoll and D. M. Healy, "Computing fourier transform and convolutions on the 2-sphere," *Advances Applied Math.*, vol. 15, pp. 202–250, 1994.
[19] S. W. Ellingson and W. Cazemier, "Efficient multibeam synthesis with interference nulling for large arrays," *IEEE Trans. Antennas Propag.*, vol. 51, pp. 503–511, Mar. 2003.
[20] S. Rao, D. Wilton, and A. Glisson, "Electromagnetic scattering by surfaces of arbitrary shape," *IEEE Trans. Antennas Propag.*, vol. 30, pp. 409–418, May 1982.
[21] R. Mittra, J-F. Ma, E. Lucente, and A. Monorchio, "CBMOM—an iteration free MoM approach for solving large multiscale EM radiation and scattering problems," presented at the Proc. IEEE Symp. Antennas Propagat. Soc., Washington, DC, Jul. 3–8, 2005.

Efficient Computation of the Effect of Wire Ends in Thin Wire Analysis

A. Heldring, E. Ubeda, and J. M. Rius

***Abstract*—Computationally efficient algorithms are presented for the computation of the effect of flat wire ends (end caps) in the common thin wire model. A uniform charge distribution over the surface of the end cap is assumed, and the full or exact kernel of the electric field integral equation formulation for cylindrical wires is used. The algorithms have been implemented in a highly efficient, low order, full kernel method of moments code for the analysis of relatively thick wire antennas and scatterers. The extra computational cost of including the end cap effect is small. The code has been applied to the analysis of a thick linear dipole and the results correspond very well with those of a recently published study using a much more computationally expensive implementation of the magnetic field integral equation with high order discretization methods.**

***Index Terms*—End caps, exact kernel, thin wire model.**

I. INTRODUCTION

In the thin wire formulation of the method of moments (MoM), commonly used for the analysis of wire antennas and scatterers [1], the structure under analysis is modeled as a set of short straight wire segments that only support axial surface currents, an assumption which is valid when the wire radius a is much smaller than the wavelength, $a \ll \lambda$. If the geometry allows it, the segment length Δ can be chosen large compared to the wire radius, $\Delta \gg a$, and the reduced kernel approximation can be used, in which the boundary condition that yields the electric field integral equation (EFIE) is enforced on the wire axis instead of on the wire surface. In most practical cases, good results are obtained with the reduced kernel.

However, there are certain problems of interest, where the thin wire condition $a \ll \lambda$ is complied with, but, due to the fine structure of the antenna geometry, some or most segments are necessarily shorter, sometimes even much shorter, than the wire radius. Examples of such structures are fractal antennas [3] and metamaterials [4]. In this case, the thin wire model with the full or exact kernel must be used. Evaluating the exact kernel by numerical integration or using the truncated series proposed in [5] and [6] is computationally expensive. We have recently proposed an efficient method to implement the thin wire model for arbitrarily short segments, using the full or exact kernel [7] and low order (overlapping triangular) basis and testing functions. This method permits efficient evaluation of the potentials, anywhere in space, from a linear surface current and constant surface charge on an arbitrarily

Manuscript received July 26, 2005; revised April 28, 2006.

The authors are with the Department of Signal Processing and Telecomm, Universitat Politecnica de Catalunya, 08034 Barcelona, Spain (e-mail: heldring@tsc.upc.edu).

Digital Object Identifier 10.1109/TAP.2006.882194

short cylinder, with a maximum relative error of 10^{-4}. The computational cost is approximately twice that of the reduced kernel.

As already noted by Kolundzjia [8], when the wires under analysis are relatively thick (a in the order of $\lambda/100 - \lambda/10$), one can not neglect the effect of the wire structure extremities, or end caps. These are commonly considered as flat circular disks and a physical model with a uniform charge distribution is adopted, for example in [2], [9] and [10]. However, none of these authors use the exact kernel of integration, tested on the wire surface. In [2], the current on the wire is assumed to be concentrated on the wire axis. This was shown in [11] to be equivalent to using the reduced kernel. In [9], the reduced kernel is used directly. The method of [10] also reduces to the reduced kernel when applied to perfectly conducting wires.

In this paper, we introduce a computationally efficient method to evaluate the potentials due to the end caps, with a maximum relative error of 10^{-4} anywhere in space, and using the exact kernel. The computational cost is approximately the same as that of the cylindrical kernel in [7]. This allows us to include a basis function in the MoM impedance matrix that bends over the edge with the end cap and vanishes at the end cap center. The new algorithm improves the accuracy of the MoM solution at the cost of only one additional basis function per end cap. The results agree very well with recently published high order, high accuracy results for a linear dipole [12].

II. End Cap Model

Due to symmetry there is no azimuthal surface current density component on the end cap and the radial component J_ρ has no azimuthal dependence. Furthermore, following [8], we assume a linear radial dependence of the end cap current equal to

$$J_\rho(\rho) = -\frac{\rho}{a} J_0 \tag{1}$$

where J_0 is the magnitude of the current density crossing the end cap edge. The corresponding surface charge density

$$\sigma_{ec} = \frac{j}{\omega} \nabla \cdot \overrightarrow{J} = \frac{-2j}{\omega a} J_0 \tag{2}$$

is a constant. Consequently, the scalar potential is given by

$$\Phi(\overrightarrow{r}) = \frac{\sigma_{ec}}{4\pi\varepsilon} \int_D \frac{e^{-jkR}}{R} ds', \quad R = |\overrightarrow{r} - \overrightarrow{r}'|, \tag{3}$$

where the surface D is a flat circular disk of radius a representing the end cap and $\overrightarrow{r}$ is an arbitrary point in space. Because of the $1/R$ dependence, (3) is difficult to evaluate with a high accuracy especially for small values of R. Using a kernel splitting, and noting the rotational symmetry, we rewrite (3) as

$$\Phi(\rho, z) = \frac{\sigma_{ec}}{4\pi\varepsilon} \left(\Phi(\rho, z) + \Psi(\rho, z)\right) \tag{4}$$

$$\Phi(\rho, z) = \int_D \frac{1}{R} ds' \tag{5}$$

$$\Psi(\rho, z) = \int_D \frac{e^{-jkR} - 1}{R} ds' \tag{6}$$

in a cylindrical coordinate system (ρ, ϕ, z) centered on the disk D, with D in the plane $z = 0$ and with

$$R = \sqrt{z^2 + \rho^2 + \rho'^2 - 2\rho\rho' \cos(\phi')}. \tag{7}$$

$\Psi(\rho, z)$ varies smoothly for all R and can be evaluated efficiently by numerical integration. For a relative error smaller than 10^{-4}, one point integration suffices for small radii ($a < 0.01\lambda$) and 7 point integration ([13, §25.4.61]) otherwise. Section III deals with efficient evaluation of $\Phi(\rho, z)$.

The vector potential due to (1) is given by (the hat denotes a unit vector)

$$\overrightarrow{A}(\overrightarrow{r}) = \frac{\mu}{4\pi} \int_D J'_\rho \widehat{\rho}' \frac{e^{-jkR}}{R} ds'. \tag{8}$$

The only non-negligible contribution of $\overrightarrow{A}$ is that of the end cap self-interaction. This is because near the end caps, the wire segments are generally (almost) perpendicular to the end cap surface, and they only carry axial current, which is not affected by a perpendicular vector potential. Further away, the integral in (8) partly cancels out because of the rotational symmetry of the end cap current. For the self-interaction, we use the same kernel splitting as for Φ, [(4)–(6)]. The regular term can be integrated numerically in the same way as $\Psi(\rho, z)$ above. The $1/R$-term, when tested with basis- and testing functions both defined by (1), (Galerkin's method), results in an impedance matrix contribution equal to

$$Z'_{ec} = \frac{-j\omega\mu}{4\pi a^4} \int_D \int_D \frac{\rho'\rho\cos\phi'}{R} ds' ds \tag{9}$$

which is easily shown to be proportional to a and, after numerical integration, yields $Z'_{ec} = -j\omega\mu a \times 6.7547\ \mathrm{m}\Omega$.

III. End Cap Scalar Potential

In this section we look for efficient expressions for $\Phi(\rho, z)$ for radius $a = 1$. The solution for arbitrary a follows trivially using the scaling $\Phi(\rho, z, a) = a\Phi(\rho/a, z/a, 1)$. Apart from a negative constant, $\Phi(\rho, z)$ is equivalent to the gravitational potential of a homogeneous flat disk of radius one, $V_{grav1}(\rho, z)$. Lass and Blitzer [14] published the exact solution for this potential in terms of the complete elliptic integrals of the first, second and third kind, $K(k)$, $E(k)$ and $\Pi(n^2, k)$ respectively

$$V_{grav1}(\rho, z) = \pi|z| - pE(k) - \frac{1-\rho^2}{p} K(k) - \frac{1-\rho}{1+\rho} \frac{z^2}{p} \Pi(n^2, k), \quad 0 < \rho < 1, \quad z > 0 \tag{10}$$

with $p^2 = z^2 + (1+\rho)^2$, $k^2 = 4\rho/p^2$ and $n^2 = 4\rho/(1+\rho)^2$. For $\rho > 1$, (10) also applies, but with the $\pi|z|$-term removed. The three elliptic integrals are computed to machine precision by internal functions in both the Mathematica and the Matlab computer programs. However, these implementations are unacceptably slow for our purpose. In many practical cases the bulk of the computational burden would be on the end cap element computations (see Table I). We therefore propose the more efficient approach explained below. $E(k)$ and $K(k)$, can be very efficiently evaluated using the polynomial approximations by Hastings [15] with a relative error smaller than 10^{-4}. No such approximation exists for $\Pi(n^2, k)$. However, Carlson gives an efficient iterative algorithm for the numerical evaluation of $\Pi(n^2, k)$ [16]. The algorithm is presented with a stopping criterium for a given maximum relative error. However, since our interest is the total relative error of the sum of approximated functions in (10), we investigated this total error numerically over a given domain, for a fixed number of iterations m. When $m = 2$, inside the domain given by $0 < z < 1, 0 < \rho < 2$, the maximum relative error is smaller than 10^{-4}, as required. The accuracy decreases for points further away. The reason is that the individual terms on the right hand side of (10) do not decrease with the distance, while their sum does decrease. Consequently, the total relative error (or the

TABLE I
RELATIVE COMPUTATIONAL TIMES

Method	Timing
Eq. (12), this paper (1)	1 (arbitrary units)
Eq. (10), this paper (1)	15
Eq. (10), Mathematica built-in	300
Eq. (10), Matlab (symbolic toolbox)	16700
Exact cylindrical kernel from [7] (1)	2.5
(1) Implemented in Matlab	

number of iterations for a fixed error) increases with the distance. The approach based on (10), with two iterations of the Carlson algorithm is therefore used only for calculating the field in the immediate proximity of the end cap, in the region $0 < z < 1, 0 < \rho < 2$. Outside this region we propose an approximation based on a geometrical body that is very similar to the homogeneous flat disk, and for the potential of which a simple analytical expression is available, the infinitely flattened homoeoid [17]. With the homoeoid centered in the plane $z = 0$, the potential function is given by

$$V_A(\rho, z) = C \arcsin\left(\frac{2A}{\sqrt{z^2+(\rho+A)^2}+\sqrt{z^2+(\rho-A)^2}}\right) \quad (11)$$

where A is the radius of the homoeoid in the plane $z = 0$ and C is a constant. Equating (11) and (5) asymptotically (for large ρ and z) yields $C = \pi/A$ (11) fails as an approximation to $\Phi(\rho, z)$ in the vicinity of the disk, because the mass (or charge) per unit of surface is not uniform over the homoeoid. A\ better approximation is obtained with a "hollow" homoeoid, constructed by subtracting a second, concentric homoeoid, or, more generally, a linear combination of two concentric homoeoids, maintaining the asymptotic fit to (5)

$$V_{grav2}(\rho, z) = V_{A_1} + D\,(V_{A_1} - V_{A_2})\,. \quad (12)$$

Using a nonlinear least squares fit to 10 points evenly distributed on the section $z > 0, \rho > 0$ of the ellipse $z^2 + (\rho/2)^2 = 1$, we find $A_1 = 0.939692$, $A_2 = 0.536584$ and $D = -0.22356$, and the accuracy criterion of a relative error smaller than 10^{-4} is reached for all $\rho > 1.5$ or $z > 0.75$. Combining this result with that of (10) for the very near interactions, we have a solution that complies with the accuracy criterion for any point in space. Table I gives the relative computational efficiency of the proposed methods. The relative timing for the cylindrical kernel from [7] is added for comparison. The Matlab and Mathematica results are higher precision, but this is redundant for our application. Neither program allows the user to define the precision for the elliptic integrals.

IV. LINEAR DIPOLE

In order to assess the accuracy of our model, we have applied it to the analysis of a thick linear, centerfed half wave dipole. We compare our results to those of a recently published thorough study of this problem using the MFIE and high-order solution methods [12]. The dipole has a length d, it is excited by a magnetic frill radiating at a wavelength $\lambda = 2d$ and located at the center of the dipole. The radius of the dipole is $a = 0.0625\lambda$. The magnetic frill has an inner radius equal to the dipole radius a and an outer radius $b = 1.2a$. The expression of the field of the magnetic frill can be found in [12]. Care must be taken when testing this field with the bilinear basis functions. We observed convergent results when using 2 point Gauss Legendre quadrature for testing on all the segments except the two segments on either side of the frill. For those we needed to use 20 point Gauss Legendre quadrature.

TABLE II
HALF WAVE DIPOLE ADMITTANCE

	$\Delta_{\min}$ (1)	$Y(mS)$	diff (2)
ref. [12]		$9.9184 + 3.6597j$	-
this paper			
$N = 40$	2.29	$9.9385 + 3.6525j$	0.20
$N = 80$	1.06	$9.9335 + 3.6595j$	0.14
$N = 160$	0.51	$9.9315 + 3.6613j$	0.12
$N = 320$	0.25	$9.9307 + 3.6615j$	0.12
$N = 640$	0.12	$9.9303 + 3.6616j$	0.11
no end caps		$10.5029 + 3.6749j$	5.5
(1) length of shortest segments ($\times 10^{-3}\lambda$).			
(2) relative difference with [12] ($\times 10^{-2}$).			

A. Segmentation

Using overlapping triangular basis functions, there is no reason whatsoever to use a uniform segmentation. Indeed, using the a priori knowledge that the solution will exhibit non-smooth behaviour at the feed point, because of the singularity in the incident field, and at the end caps, because of the singularity in the geometry, it is reasonable to choose a fine discretization near those points and coarser elsewhere. We also incorporate the symmetry of the problem, by choosing a segmentation that is symmetric about $z = 0$. With the above characteristics in mind, we chose a generating mesh of N' points distributed uniformly on the interval [0,3], took the natural base exponent of these points, scaled the resulting set onto [0,0.125] and built the final mesh out of four, adequately arranged copies of this set. The resulting final mesh then consists of $N = 4(N' - 1)$ segments.

B. Driving Point Admittance

In accordance with [12], we computed the driving point admittance $Y = 2\pi a J_z/V|_{z=0}$, with V, the feeding voltage set equal to 1 V. In order to assess the convergence of the method with respect to the discretization, we repeated the computation for a range of values of N (see previous section). We also computed Y without including the end caps, for comparison. The results and their comparison to the result reported in [12] are shown in Table II.

Table II shows that the approach of this paper converges to a residual difference with the reference of 0.11%. This difference is caused by the principal approximation in our model, which is to assume a perfectly constant charge density on the end cap. In [12] the end cap is further discretized, and their results show that although the charge density is approximately constant over most of the end cap, there is a sharp peak towards the edge, due to the singularity in the geometry. If we wanted to include this in our model, we would have to compute the potentials for mutual interaction between distinctive basis functions on the end cap, for which efficient algorithms like those of Section III are unavailable. This would destroy the high efficiency which characterizes our method.

Fig. 1 shows the conductance $G = \mathrm{Re}\{Y\}$ for a half wave dipole, computed using the approach of this paper with and also without including the end caps, as a function of the wire radius a. The feeding is the same as above, and we used $N = 640$. The results are compared to those of [12, Fig. 5]. The susceptance $G = \mathrm{Im}\{Y\}$ is not shown because the difference between the four graphs is negligible. As expected, the effect of the end caps grows with the wire radius. Table III gives the results with the end caps and the relative difference with [12] for a number of wire radii. The fact that the difference starts growing again below a certain wire radius, is possibly because the current drops steeper near the end cap for smaller a, which is harder to capture with linear basis functions.

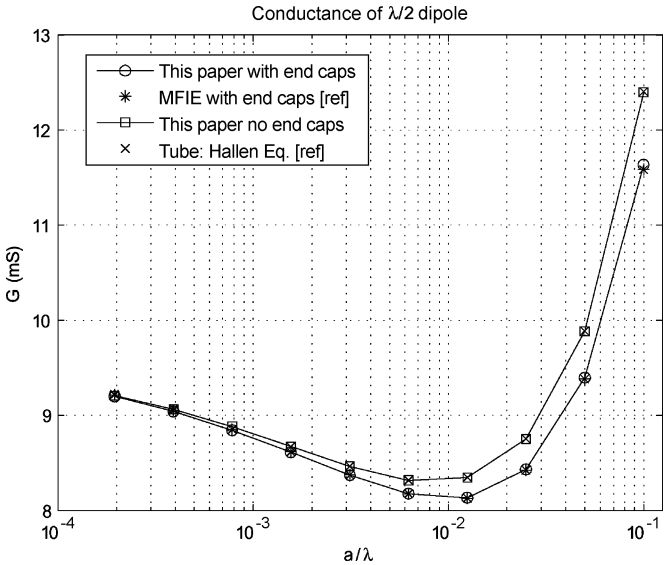

Fig. 1. Conductance of half wave dipole as a function of wire radius a. The reference data are from [12].

TABLE III
HALF WAVE DIPOLE ADMITTANCE

wire radius a/λ	$Y(mS)$	diff [1]
0.1	$11.6012 + 6.8476j$	0.12
0.025	$8.4327 - 0.4191j$	0.07
6.25×10^{-3}	$8.1783 - 3.4363j$	0.03
1.56×10^{-3}	$8.6140 - 4.6439j$	0.05
3.91×10^{-4}	$9.0410 - 5.1264j$	0.12
[1]relative difference with [12] ($\times 10^{-2}$)		

V. CONCLUSION

Fast and accurate algorithms for the potential of a uniform charge distribution on a flat cylinder have been presented. They were implemented in a low order, and therefore computationally efficient, full kernel thin wire code, based on the EFIE, to model the charge accumulation on the wire end caps. A range of linear dipoles with varying wire radius and a fixed length of $\lambda/2$ was analysed and the results showed good correspondence with those of a recent high order MFIE model from the literature. It is further noteworthy that, in spite of the linear discretization, even a 40 segment model showed quite accurate results (0.2% difference with the reference). The latter model has 39 bilinear cylindrical basis functions plus two end caps, amounting to 41 unknowns in total.

ACKNOWLEDGMENT

The authors would like to thank the authors of [12] for giving them the necessary data for Fig. 1 and Table III.

REFERENCES

[1] R. F. Harrington, *Field Computation by Moment Methods*. New York: MacMillan, 1968.
[2] B. D. Popovic, M. B. Dragovic, and A. R. Djordjevic, *Analysis and Synthesis of Wire Antennas*. Chichester, U.K.: U.K. Research Studies Press, 1982.
[3] C. Puente, J. Romeu, R. Pous, J. Ramis, and A. Hijazo, "Small but long Koch fractal monopole," *IEE Electron. Lett.*, vol. 34, no. 1, pp. 9–10, Jan. 1998.
[4] E. Ozbay, K. Aydin, E. Cubukcu, and M. Bayindir, "Transmission and reflection properties of composite double negative metamaterials in free space," *IEEE Trans. Antennas Propag.*, vol. 51, no. 10, pp. 2592–2595, Oct. 2003.
[5] S. Park and C. Balanis, "Efficient kernel calculation of cylindrical antennas," *IEEE Trans. Antennas Propag.*, vol. 43, no. 11, Nov. 1995.
[6] D. H. Werner, "A method of moments approach for the efficient and accurate modeling of moderately thick cylindrical wire antennas," *IEEE Trans. Antennas Propag.*, vol. 46, no. 3, pp. 373–382, Mar. 1998.
[7] A. Heldring and J. M. Rius, "Efficient full-kernel evaluation for thin wire analysis," *Microw. Opt. Technol. Lett.*, vol. 44, no. 5, pp. 477–480, March 2005.
[8] B. M. Kolundzija, "Effect of a wire end in thin-wire analysis," in *AP-S Digest*, 1988, vol. 2, pp. 843–846.
[9] C. D. Taylor and D. R. Wilton, "The extended boundary condition solution of the dipole antenna of revolution," *IEEE Trans. Antennas Propag.*, vol. 20, no. 6, pp. 772–776, Nov. 1972.
[10] E. H. Newman, "A unified theory of thin material wires," *IEEE Trans. Antennas Propag.*, vol. 39, no. 10, Oct. 1991.
[11] A. G. Tijhuis, P. Zhongqiu, and A. Rubio Bretones, "Transient excitation of a straight thin wire segment: a new look at an old problem," *IEEE Trans. Antennas Propag.*, vol. 40, no. 10, Oct. 1992.
[12] A. F. Peterson and M. M. Bibby, "High order numerical solutions of the MFIE for the linear dipole," *IEEE Trans. Antennas Propag.*, vol. 52, no. 10, pp. 2684–2991, Oct. 2004.
[13] M. Abramowitz and I. A. Stegun, Eds., Handbook of Mathematical Functions 9th printing New York, Dover, 1972.
[14] H. Lass and L. Blitzer, "The gravitational potential due to uniform disks and rings," *Celestial Mechanics*, vol. 30, pp. 225–228, 1983.
[15] C. Hastings, *Approximations for Digital Computers*. Princeton, NJ: Princeton Univ. Press, 1955.
[16] B. C. Carlson, "Numerical computation of real or complex elliptic integrals," *Numerical Algorithms*, vol. 10, pp. 13–26, 1995.
[17] J. Binney and S. Tremaine, *Galactic Dynamics*. Princeton, NJ: Princeton Univ. Press, 1987.

Polar Integration for Exact Space-Time Quadrature in Time-Domain Integral Equations

James Pingenot, Swagato Chakraborty, and Vikram Jandhyala

***Abstract*—A space-time polar quadrature technique for numerical integration of Green's function interactions in time-domain integral equations is presented. The method transforms 2-D surface space-time integrals associated with vector and scalar potentials to a 1-D integral that is performed using Gauss-Legendre integration. The advantage of the presented technique compared to standard 2-D Gaussian quadrature is that time delays between each section of the source basis function and the observation point are accounted for exactly in an analytic manner. This ensures highly accurate temporal behavior of the Green's function interactions thereby contributing to the stability of the overall time-domain integral equations.**

***Index Terms*—BEM, integral equations, integration, quadrature, time domain.**

I. INTRODUCTION

Time-domain integral equations (TDIEs) are now powerful and rapidly evolving tools for temporal simulation of electromagnetic behavior of complex structures. Several researchers have recently developed techniques for enhancing stability. In addition to techniques for stability such as special basis functions [1]–[3] and implicit schemes [4], it is also imperative to have accurate space-time quadrature schemes. Compared to frequency-domain quadrature, TDIE integration has the additional property of requiring exact time delays

Manuscript received August 22, 2005; revised April 16, 2006.
The authors are with the Electrical Engineering Department, University of Washington, Seattle, WA 98105 USA (e-mail: pingej@u.washington.edu).
Digital Object Identifier 10.1109/TAP.2006.882195